

# PrecoG: an efficient unitary split preconditioner for the transform-domain LMS filter via graph Laplacian regularization

Tamal Batabyal\*, Daniel S. Weller, Scott T. Acton

*Department of Electrical and Computer Engineering, University of Virginia,  
Charlottesville-22904, Virginia, United States*

---

## Abstract

Transform-domain least mean squares (LMS) adaptive filters encompass the class of algorithms in which the input data are subjected to a unitary transform followed by a power normalization stage and an LMS adaptive filter. Because of the data-independent nature of conventional transformations, such a transformation improves the convergence of the LMS filter only for certain classes of input data. However, for input data from unknown classes or a specific set of classes, it is difficult to decide which transformation to use. This decision necessitates a learning framework that obtains such a transformation using input data, which improves the condition number after transformation with minor additional computation. It is hypothesized that the underlying data topology affects the selection of the transformation. With the data modeled as a weighted graph and the input autocorrelation matrix known or computed beforehand, we propose a method, PrecoG, that obtains the desired transform by recursively estimating the graph Laplacian matrix. Additionally, we show the efficacy of the transformation as a generalized split preconditioner on a linear system of equations with an ill-conditioned real positive definite matrix. PrecoG shows significantly improved post-transformation condition number as compared to the existing state-of-the-art techniques that involve unitary and non-unitary

---

\*Corresponding author Tel.: +1-434-466-5486; fax: +1-434-924-8818;  
*Email address:* [tb2ea@virginia.edu](mailto:tb2ea@virginia.edu) (Tamal Batabyal)

transforms.

*Keywords:* graph Laplacian, regularization, split preconditioner, LMS filter, unitary transform

---

## 1. Introduction

In 1960, Bernard Widrow and Ted Hoff [1] proposed a class of *least mean squares* (LMS) algorithms to recursively compute the coefficients of an N-tap finite impulse response (FIR) filter that minimizes the output error signal. This computation is achieved by a stochastic gradient descent approach where the filter coefficients are evaluated as a function of the *current error* at the output. Two of the major issues with this approach are the convergence speed and stability. The filter coefficients (or weights) converge in mean while showing small fluctuation in magnitude around the optimal value. The convergence speed depends on the condition number of the autocorrelation matrix of the input, where a condition number close to unity connotes a fast and stable convergence. Later, adaptive algorithms, such as LSL (least square lattice) and GAL (gradient adaptive lattice) [2, 3] filters were designed to achieve faster convergence, immunity to poor condition number of input autocorrelation matrix, and better finite precision implementation compared to the LMS filter. However, these stochastic gradient filters may sometimes produce significant numerical errors, and the convergence is poor compared to recursive least squares (RLS) filters [4].

In order to obtain well-conditioned autocorrelation matrix of any real world input data, we transform the input *a priori*, which is popularly known as transform-domain LMS (TDLMS). The discrete Fourier transform (DFT), discrete cosine transform (DCT) [5, 6, 7, 8] and others act as suitable off-the-shelf transformations of the input data for such problems. The aforementioned step is immediately followed by a power normalization stage [9, 10] and then used as input to the LMS filter. As a geometrical interpretation, the unitary transformation rotates the mean square error (MSE) hyperellipsoid without changing its shape on the axes of LMS filter weights [10]. The rotation tries to align the

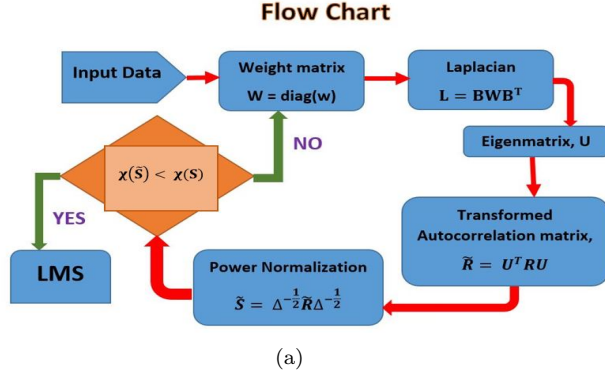


Figure 1: A schematic of our algorithm.

axes of the hyperellipsoid to the axes of weights. The power normalization is crucial in enhancing the speed of convergence of LMS filter. The normalization forces the hyperellipsoid to cross all the axes at equal distance from the center of the hyperellipsoid. For a perfect alignment after the transformation, the normalization step turns the MSE hyperellipsoid into a hypersphere [10].

The TDLMS filter is flexible as it does not attempt to change the working principles and the architecture of LMS filter. Therefore, the transform-domain module can precede other algorithms, such as RLS, GAL and LSL. Notice that the conventional unitary transformations are independent of the underlying data, hence not optimal in regularizing condition numbers of the autocorrelation matrices of arbitrary real-time datasets. As an example, the DCT has been shown to be near-optimal for Toeplitz matrices. However, the DCT loses its near-optimality in conditioning sparse linear systems.

From a different perspective, the transformation of a matrix, such as autocorrelation matrix to improve the condition number is regarded as a subproblem of preconditioning of matrices [11, 12, 13, 14]. Jacobi [15, 16], Gauss-Seidel [17], approximate inverse [18, 19], incomplete LU factorization [20] preconditioners are examples of such data-dependent transformations that utilize a decomposition of the input autocorrelation matrix. These algorithms are well-suited for solving linear system of equations.

Notice that there is a difference between TDLMS and linear systems in terms of the usage of a preconditioner. The preconditioning action is *implicit*

in TDLMS filters. The autocorrelation matrix is not explicitly used in the LMS architecture. Instead, it is the input data or the transformed input data (in case, we transform the data) that flows through the LMS lattice and the update of weights is based on error-correcting learning. The convergence of the algorithm depends on the input autocorrelation matrix. Whereas, in case of solving linear system of equations, ( $Ax = b$ ) type, the use of a preconditioner is *explicit*, which is  $M^{-1}Ax = M^{-1}b$ , with  $M$  as a preconditioner matrix, such as the Gauss-Seidel type.

Let  $A$  be a matrix to be preconditioned by another matrix  $\zeta$ .  $\zeta$  is said to be a left, right, and split preconditioner if  $\zeta^{-1}A$ ,  $A\zeta^{-1}$ , and  $U_1^{-1}AU_2^{-T}$  with  $\zeta = U_1U_2^T$  respectively provide improved condition numbers compared to that of  $A$ . Gauss-Seidel, incomplete LU, and approximate inverse are examples of a left preconditioner. The transformations in TDLMS algorithm are the unitary split preconditioner type. By unitary, we have ( $U_1U_2^T = I$ ) and  $U_1 = U_2 = U$ .

In PrecoG, we aim to learn such unitary split preconditioner from input data. It is because unlike a left or right preconditioner, the operation of a split preconditioner entails the possibility of a *transformation of input data* in which the input data vector is left-multiplied by  $U^T$ . It is the split preconditioner which helps apply PrecoG to TDLMS as well as solving a linear system of equations, and possibly any applications where preconditioner or transformation is needed. There are additional benefits of this approach. As the transformation is unitary, the energy of input data remains unchanged after transformation. In addition, the procedure of preconditioning that transforms the input vector as an intermediate step can utilize a number of input signal properties (e.g., the sparsity of a signal).

The derivation of our split conditioner is motivated by the topology of the structured input data. The topology determines neighborhood relationship between data points, which can be represented using graph-theoretic tools [21, 22, 23]. In recent years, manifold processing and regularization have shown promise in different areas of research [24, 25, 26, 27]. Based on such evidence, we hypothesize that the intrinsic topology of the input data affects the construction

of a suitable preconditioner matrix. We estimate a data manifold that provides an alternate set of basis acting as a split preconditioning matrix. The data when projected onto the basis are expected to be decorrelated.

The *main contribution* of this work is to provide an *optimization* framework that finds the desired unitary transformation for the preconditioning matrix. We iteratively estimate the underlying topology leveraging graph theory, followed by the computation of desired unitary transformation by using the graph Laplacian. Most importantly, we show that our approach is equally applicable in preconditioning arbitrary linear systems apart from ameliorating the convergence of LMS filters. In addition, PrecoG can be extended to exploit additional input data constraints, such as sparsity of the transformed input. Another advantage of PrecoG is that it can be applied without having a prior knowledge about the process that generates the input data.

## 2. Graph Theory

A graph can be compactly represented by a triplet  $(\mathcal{V}, \mathcal{E}, \mathbf{w})$ , where  $\mathcal{V}$  is the set of vertices,  $\mathcal{E}$  the set of edges, and  $\mathbf{w}$  the weights of the edges. For a *finite* graph,  $|\mathcal{V}| = N$  which is a finite positive integer, and  $|\bullet|$  is the cardinality of a set. By denoting  $w_{ij} \in \mathbf{w}$  as a real positive weight between two vertices  $i$  and  $j$  with  $i, j \in \{1, 2, \dots, N\}$ , the adjacency matrix,  $A$  of  $\mathcal{G}$  can be given by  $a_{ij} = w_{ij}$  with  $a_{ii} = 0$  for a graph with no self-loop.  $A \in \mathcal{R}^{N \times N}$  is symmetric for an undirected graph and can be sparse based on the number of edges. The incidence matrix,  $B \in \mathcal{R}^{N \times |\mathcal{E}|}$  of  $\mathcal{G}$  is defined as  $b_{ij} = 1$  or  $-1$  where the edge  $j$  is incident to or emergent from the vertex  $i$ . Otherwise  $b_{ij} = 0$ . The graph Laplacian  $L \in \mathcal{R}^{N \times N}$ , which is a symmetric positive-semidefinite matrix, can be given by  $L = BWB^T$ , where  $W$  is a diagonal matrix containing  $\mathbf{w}$ . Determining the topology of input data refers to the estimation of  $A$  or  $L$  depending on the formulation of the problem at hand.

## 3. Problem statement

Let  $x_k = [x(k) \ x(k-1) \ \dots \ x(k-N+1)]$  be a  $N$ -length real valued tap-delayed input signal vector at  $k^{th}$  instant. The vector representation is convenient for

estimating the input autocorrelation as an ergodic process. Let the autocorrelation matrix, denoted by  $R_N$  be defined as  $R_N = E(x_N x_N^T)$ . We assume that  $\Delta_Y$  is the main diagonal of a square matrix  $Y$  ( $\Delta_Y = \text{diag}(Y)$ ). Following this notation, after power normalization the autocorrelation matrix becomes  $S_N = \Delta_{R_N}^{-\frac{1}{2}} R_N \Delta_{R_N}^{-\frac{1}{2}}$ . In general, the condition number of  $S_N$ ,  $\chi_{S_N}$ , happens to be significantly large in practical datasets. For example, the condition number of the autocorrelation matrix of a Markov process with signal correlation factor as 0.95 has a  $\chi$  of  $\mathcal{O}(10^3)$ . Notice that we seek  $U_N$  to minimize the condition number of  $S_N$ . Let a unitary transformation be  $U_N$  ( $U_N U_N^T = I$ ) such that the transformed autocorrelation matrix becomes  $\tilde{R}_N = E[U_N^T x_k x_k^T U_N]$ . Next,  $\tilde{R}_N$  is subjected to a power normalization stage that produces  $\tilde{S}_N = \Delta_{\tilde{R}_N}^{-\frac{1}{2}} \tilde{R}_N \Delta_{\tilde{R}_N}^{-\frac{1}{2}}$ . Precisely, we want the eigenvalues of  $\lim_{N \rightarrow \infty} \tilde{S}_N \in [1 - \epsilon_2, 1 + \epsilon_1]$ , where  $\epsilon_1$  and  $\epsilon_2$  are arbitrary constants such that  $\chi_{max} \simeq \frac{1+\epsilon_1}{1-\epsilon_2}$ . A schematic of our algorithm is given in Fig. 1.

Let us take an example of a 1<sup>st</sup> order Markov input with the signal correlation factor  $\rho$  and autocorrelation matrix,  $R_N$  as

$$R_N = E[\mathbf{x}_k \mathbf{x}_k^H] = \begin{pmatrix} 1 & \rho & \dots & \rho^{n-1} \\ \rho & 1 & \dots & \rho^{n-2} \\ \vdots & \vdots & \ddots & \vdots \\ \rho^{n-1} & \rho^{n-2} & \dots & 1 \end{pmatrix} \quad (1)$$

It is shown in [10] that  $\chi_{S_N} \simeq (\frac{1+\rho}{1-\rho})^2$ , which suggests that  $\epsilon_1 = \rho^2 + 2\rho$ , and  $\epsilon_2 = 2\rho - \rho^2$ . After applying the DFT, the condition number becomes  $\lim_{N \rightarrow \infty} \chi_{\tilde{S}_N} = (\frac{1+\rho}{1-\rho})$ , which indicates that  $\epsilon_1 = \epsilon_2 = \rho$ . On applying the DCT,  $\lim_{N \rightarrow \infty} \chi_{\tilde{S}_N} = 1 + \rho$  with  $\epsilon_1 = \rho$  and  $\epsilon_2 = 0$ .

#### 4. Methodology

The search for  $U_N$  is carried out through an iterative optimization of an associated cost function. It can be argued from section 3 that the optimal convergence properties are obtained when  $\tilde{S}_N$  converges to the identity matrix

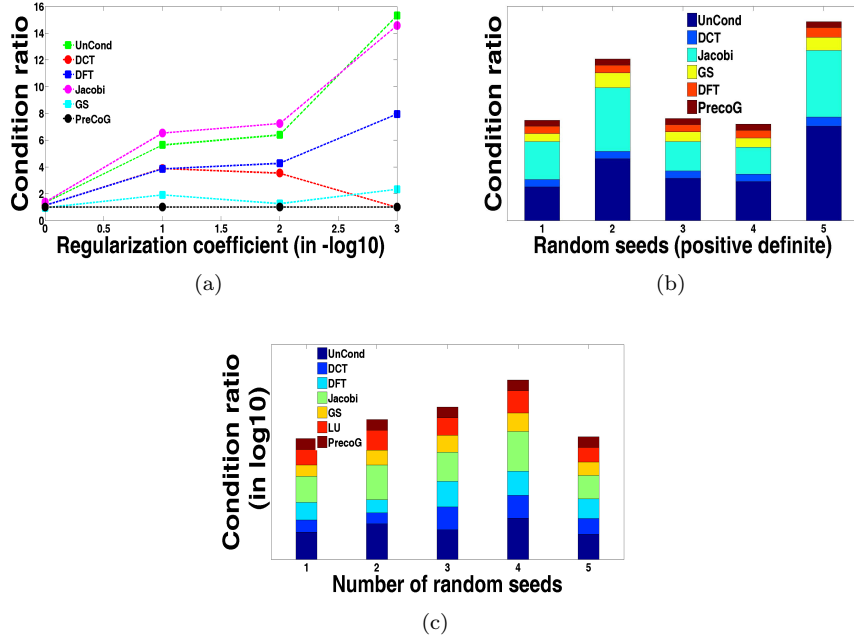


Figure 2: Condition ratios obtained by applying the algorithms on (a) regularized Hilbert matrices with varied regularization parameters, (b) a set of random matrices containing entries  $\sim \text{Gaussian}(0, 1)$ , and (d) random matrices of varied sparsities (for sparse linear systems).

in the *rank zero perturbation* sense [10]:  $A$  and  $B$  with  $\eta = A - B$  have the same asymptotic eigenvalue distribution if

$$\lim_{N \rightarrow \infty} \text{rank}(\eta) = 0. \quad (2)$$

In our case, with  $\lambda$  as an eigenvalue, this translates to

$$\lim_{N \rightarrow \infty} \det(\tilde{S}_N - \lambda \mathbb{I}_N) = 0, \quad (3)$$

which can be expanded as,

$$\lim_{N \rightarrow \infty} \det\left(\Delta_{\tilde{R}_N}^{-1/2} \tilde{R}_N \Delta_{\tilde{R}_N}^{-1/2} - \lambda \mathbb{I}_N\right) = 0. \quad (4)$$

Eq. (4) can be rearranged as,

$$\lim_{N \rightarrow \infty} \det\left(\tilde{R}_N - \lambda \Delta_{\tilde{R}_N}\right) = 0, \quad (5)$$

which is a quadratic polynomial of  $U_N$  as  $\tilde{R}_N = U_N^T R_N U_N$ . Given the orthonormality of the eigenvectors  $U_n$ , we can rewrite (5) as

$$U_N = \operatorname{argmin}_{U_N \in O(N)} \left[ \det \left( \tilde{R}_N - \lambda \Delta_{\tilde{R}_N} \right) \right]. \quad (6)$$

Here,  $O(N)$  is the set of unitary matrices. However, in presence of the determinant in (6), obtaining a closed-form expression for  $U_N$  is difficult to obtain. To overcome this obstacle, we apply the Frobenius norm in (7).

$$U_N = \operatorname{argmin}_{U_N \in O(N)} \|\tilde{R}_N - \lambda \Delta_{\tilde{R}_N}\|_F^2. \quad (7)$$

The Frobenius norm imposes a stronger constraint compared to (3). In fact, while (5) can be solved if at least one column of  $\tilde{R}_N - \lambda \Delta_{\tilde{R}_N}$  can be expressed as a linear combination of rest of the columns, (7) becomes zero only when  $\tilde{R}_N - \lambda \Delta_{\tilde{R}_N}$  is a zero matrix. In effect, it reduces the search space of  $U_N$ . It is due to the fact that the set of  $U_N$  that solves eq. (7) is a subset of the  $U_N$  that are the solutions of eq. (6). Here, we address two aspects of the problem. First, (7) attempts to minimize the difference between  $\tilde{R}_N$ , which is  $U_N^T R_N U_N$ , and the scaled diagonal matrix of  $\tilde{R}_N$ . This is necessary because it accounts for the spectral leakage [10] as mentioned later in this section. The second aspect is that (7) seems to diagonalize  $\tilde{R}_N$  apart from attempting to make the eigenvalues unity only. Here, a solution may be hard to obtain in practice. So, we relax the unity constraint by forcing the eigenvalues to lie within a range  $[1 - \epsilon_2, 1 + \epsilon_1]$ . By enforcing the constraint, (7) with parameters  $p = (\mathbf{w}, \epsilon_1, \epsilon_2)$  becomes

$$U_N = \operatorname{argmin}_{U_N \in O(N)} \underbrace{\|\tilde{R}_N - s_+ \Delta_{\tilde{R}_N}\|_F^2 + \|\tilde{R}_N - s_- \Delta_{\tilde{R}_N}\|_F^2}_{E(p)}. \quad (8)$$

where  $s_+ = 1 + \epsilon_1$  and  $s_- = 1 - \epsilon_2$  are the upper and lower bounds respectively for the eigenvalues of  $S_N$ . Using the Hadamard product notation, we can express  $\Delta_{\tilde{R}_N}$  as  $U_N^T R_N U_N \circ \mathbb{I}_N$ . The first two constraints in (8) provide a valley in the space spanned by the eigenvectors in  $U_N$  if  $R_N$  is positive definite. The valley

exists between two surfaces  $(1-\epsilon_2)U_N^T R_N U_N \circ I$  and  $(1+\epsilon_1)U_N^T R_N U_N \circ I$ . At this point, there might be infinitely-many possible solutions. We add a regularizer on  $\mathbf{w}$  to obtain an acceptable set of solutions.

The undesired result of the imposed restriction given above is that the convergence time may be significant, and the set of solutions of (8) in terms of  $U_N$  is significantly smaller than that of (7). Upon approaching a minimum of (7), the speed of gradient descent algorithm drops significantly. Although it is theoretically expected that  $\lim_{N \rightarrow \infty} \tilde{S}_N \in [1 - \epsilon_2, 1 + \epsilon_1]$ , in practice, it is difficult to guarantee after a prescribed number of iterative steps.

### 5. Laplacian parametrization

The problem of finding a sub-optimal transform by optimizing eq. (8) is solved by leveraging the graph framework. In this framework, the input data is modeled with a finite, single-connected, simple, and undirected graph endowed with a set of vertices, edges and edge weights. For example, for an LMS filter with  $N$  taps, an input signal vector  $x_k$  has length  $N$ , which can be represented with  $N$  vertices. Basically, each vertex corresponds to one tap of the LMS filter. Using the graph, the unknowns of the optimization in (8) are the number of edges and the associated edge weights. A fully-connected graph with  $N$  vertices contains  $\frac{N(N-1)}{2}$  edges. A deleted edge can be represented with zero edge weight. We denote the the set of unknown parameters as  $\mathbf{w}$ , which is the set of nonzero weights of the graph.

To find the desired transformation, the algorithm initializes the weights  $\mathbf{w}$  with random numbers sampled from a Gaussian distribution with zero mean and unit variance. Let  $W$  is the diagonal matrix containing  $\mathbf{w}$ . Then by definition, the graph Laplacian, which is symmetric and positive semidefinite by construction, is given by  $L = BWB^T$ .  $B$  is the incidence matrix as mentioned in section 2. The spectral decomposition of  $L$  provides the matrix of eigenvectors  $U$ . Finally,  $U^T x_k$  is the transformation that is expected to decorrelate the dataset, which may not be possible due to random initialization. Then the cost function (8) helps update the weights and the search for the desired trans-

formation continues in an iterative fashion until the objective conditions are met.

The framework provides a couple of advantages. Firstly, in order to obtain  $U$  directly from eq. (8), iterative estimation of  $N^2$  parameters is needed with the unitary constraint, which might result in overfitting. Moreover it does not seem reasonable to make  $U$  sparse. Sparsification is justified in the graph domain, where the sparsifying action leads to  $\mathcal{O}(N)$  number of edges and edge weights. A smaller set of weights helps prevent the risk of overfitting during optimization.

The cost function in eq. (8) is nonconvex. Therefore, the solution is not guaranteed to be a global optimum. In our work, the required solution is obtained through gradient descent with  $\mu$  as the step size parameter. From section 2, we obtain that  $L = BWB^T$ . Let  $\Theta_i = \frac{\partial L}{\partial w_i}$ , which can be evaluated as  $\frac{\partial L}{\partial w_i} = B \frac{\partial W}{\partial w_i} B^T$ . Using  $\mu$  and  $\Theta_i$ , the update equation is given by,

$$\begin{aligned} w_i^{t+1} &= w_i^t - \mu \text{Tr} \left( \left[ \frac{\partial E(p)}{\partial U_N} \right]^T \frac{\partial U_N}{\partial w_i} \right); 0 < \mu < 1 \\ \frac{\partial u_{k,l}}{\partial w_i} &= \text{Tr} \left( \frac{\partial u_{k,l}}{\partial L} \Theta_i \right) = \text{Tr} \left( \left[ \frac{\partial L}{\partial u_{k,l}} \right]^{-T} \Theta_i \right), \end{aligned} \quad (9)$$

where, by using  $J^{mn} = \delta_{mk} \delta_{nl}$ ,  $\frac{\partial L}{\partial u_{kl}}$  can be given by,

$$L = U_N \Gamma U_N^T \implies \frac{\partial L}{\partial u_{kl}} = U_N \Gamma J^{mn} + J^{nm} \Gamma U_N^T. \quad (10)$$

In eq. (9),  $t$  is the iteration index, and the computation of  $\frac{\partial E(p)}{\partial U_N}$  is given in the Appendix. To prevent each  $w_i$  from erratic values during iteration, we impose 2-norm on the weight vector  $\mathbf{w}$ . On adding the regularization term to eq. (8), the new cost function becomes

$$E_N(\mathbf{w}, \epsilon_1, \epsilon_2, \beta) = E(p) + \beta(\mathbf{w}^T \mathbf{w} - 1). \quad (11)$$

On differentiating  $E_N$  with respect to  $\mathbf{w}$ , we get

$$\frac{\partial E_N}{\partial \mathbf{w}} = \frac{\partial E(p)}{\partial \mathbf{w}} + 2\beta \mathbf{w} \quad (12)$$

Following eq. (12), the iterative update of each weight can be given by,

$$w_i^{t+1} = w_i^t(1 - 2\beta) - \mu Tr \left( \left[ \frac{\partial E(p)}{\partial U_N} \right]^T \frac{\partial U_N}{\partial w_i} \right). \quad (13)$$

### 5.1. Complexity analysis

The update of weights  $w_i$  requires the computation of three partial derivatives (see Appendix 7). Notice that  $\frac{\partial L}{\partial u_{kl}}$  and  $\frac{\partial L}{\partial w_i}$  are significantly sparse. This can be seen from (10), where  $J^{mn}$  is a matrix containing only one nonzero entry of magnitude unity. Using the fact that  $\Gamma$  is a diagonal matrix containing eigenvalues of  $L$ ,  $\frac{\partial L}{\partial u_{kl}}$  in (10) contains at most  $(2N - 1)$  nonzero entries out of  $N^2$  entries, where  $N^2$  is the dimension of  $\frac{\partial L}{\partial u_{kl}}$ . This sparse matrix is singular by construction, and the Moore-Penrose pseudoinverse ( $\mathcal{O}(N^3)$ ) is computed in order to obtain  $\left(\frac{\partial L}{\partial u_{kl}}\right)^{-1}$ . It can also be observed that  $\frac{\partial L}{\partial w_i}$  is sparse. This sparsity is due to the fact that  $\frac{\partial L}{\partial w_i} = B \frac{\partial W}{\partial w_i} B^T$ , and each weight  $w_i$  appears in exactly four entries of  $L$ . It asserts that  $\frac{\partial L}{\partial w_i}$  has four nonzero entries out of  $N^2$  entries in  $\frac{\partial L}{\partial w_i}$ . Let  $L(k, l) = w_i$ ;  $1 \leq k, l \leq N$ . Then,  $\Theta_i(k, k) = \Theta_i(l, l) = 1$  and  $\Theta_i(k, l) = \Theta_i(l, k) = -1$ , which implies that only  $k^{th}$  and  $l^{th}$  columns of  $\Theta_i$  contain nonzero entries. Therefore,  $Tr \left( \left[ \frac{\partial L}{\partial u_{k,l}} \right]^{-T} \Theta_i \right)$  can be given by the sum of  $(k, k)$  and  $(l, l)$  entries in  $\left[ \frac{\partial L}{\partial u_{k,l}} \right]^{-T} \Theta_i$ . The lone computationally expensive operation is computation of the pseudoinverse  $\left(\frac{\partial L}{\partial u_{kl}}\right)^{-1}$ ;  $1 \leq k, l \leq N$ , which incurs in total a complexity of  $\mathcal{O}(N^5)$  for each weight. It is to note that the constructions of preconditioners for solving linear systems by comparative methods such as, Jacobi ( $\mathcal{O}(N^2)$ ), successive over-relaxation (SOR) ( $\mathcal{O}(N^3)$ ), symmetric SOR ( $\mathcal{O}(N^3)$ ), Gauss-Seidel ( $\mathcal{O}(N^3)$ ) have faster associated run times compared to PrecoG. Here, complexity accounts for the inversion of each preconditioner matrix. However, the acceleration in the convergence of the LMS filter using PrecoG is also expected to partially compensate for the computational overload of PrecoG.

### 5.2. Sparse signal and sparse topology estimation

For an input signal vector of length  $N$ , the graph can be fully connected with  $\frac{N(N-1)}{2}$  edge weights ( $\mathcal{E}$ ), which implies a dense topology. However, dense

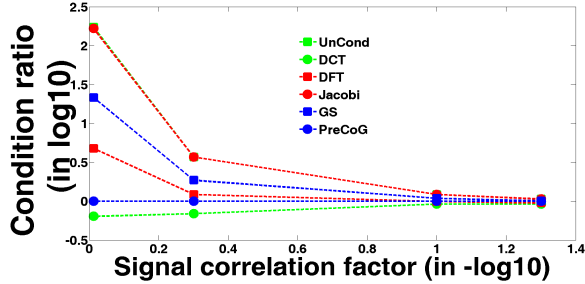
topology may lead to overfitting during the optimization using gradient descent in (9). We employ a fixed regular topology by setting the connectivity among vertices such that  $e_{ij} \in \mathcal{E}$  exists if  $0 < |i - j| \leq 2$ . This fixed topology maintains the temporal order in which the data point arrives and keep the topology sparse. The estimation of the sparse topology [28] along with the constraint of sparsity of the transformed signal can also be achieved by adding a regularization term to (11) as

$$E_N(p, \beta, \alpha_1, \alpha_2) = E_N - \alpha_1 \mathbf{1}^T \log(A\mathbf{1}) + \alpha_2 \|U_N^T x_k\|_0. \quad (14)$$

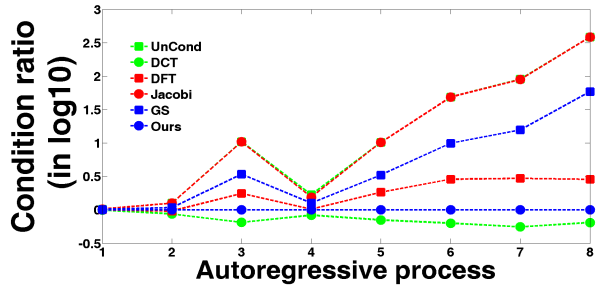
Here,  $A$  is the adjacency matrix consisting of  $\mathbf{w}$ , and  $A\mathbf{1}$  is the degree vector containing weighted degree of all the data points. By penalizing high degree vertices (data points) the  $\log$  penalty term promotes sparsity in  $A$ . On the other hand, it strongly discourages any vertex to have degree zero, maintaining the graph to be single connected. In (14),  $\|U_N^T x_k\|_0$  regulates the sparsity of the transformed signal. Such a sparse signal involves reduced multiplication with filter coefficients in the LMS filter than a non-sparse signal, which saves significant computation time. This feature can not be obtained by applying conventional transforms, such as DCT.

## 6. Results

We show the effectiveness of our approach in preconditioning different matrices against the preconditioners - DCT, DFT, Jacobi (tridiagonal matrix type) and GS (*Gauss – Seidel*). In addition, for sparse linear systems, we include a comparison with the incomplete LU factorized preconditioning procedure. It is not reasonable to compare our results with LSL, GAL, and RLS because they are the improvements of the traditional LMS algorithm. To represent the strength of an individual algorithm, we incorporate the condition number of each unconditional matrix with the aforementioned methods. In order to scale the condition numbers obtained from several methods with respect to ours, we define a metric,  $condition\ ratio = \frac{\text{condition number obtained from a method}}{\text{condition number obtained from our method}}$ . In



(a)



(b)

Figure 3: Condition ratios obtained by applying the algorithms on (a)  $1^{st}$  order Markov process as a function of signal correlation factor  $\rho$  and (b)  $2^{nd}$  order autoregressive process with parameters  $(\rho_1, \rho_2)$ .

some of the results, we compute  $\log_{10}(\text{condition ratio})$  to mitigate the enormous variance present in the condition ratio scores. First, we apply our method to precondition a Hilbert matrix [29] which is severely ill-conditioned. Hilbert matrix,  $H$  is defined as  $H(i, j) = \frac{1}{i+j-1}$ . In the experiment, we add a regularizer using  $(\alpha I)$  with  $0 < \alpha \leq 1$  as the regularization coefficient. The condition ratios of the existing algorithms including PreCoG on preconditioning the Hilbert matrices, which are regularized by changing the  $\alpha$ , are shown in Fig. 2(a). Notice that the X-axis is given in  $-\log_{10}$  scale. Therefore, smaller values at X coordinate indicates higher regularization of the Hilbert matrix. On increasing the value of  $\alpha$ , the Hilbert matrix becomes diagonally-dominant, and it suggests that the condition number of the Hilbert matrix approaches unity. This fact is clearly visible from Fig. 2(a), where all the state-of-the-art techniques including PreCoG performs significantly well when the value of  $-\log_{10}(\alpha)$  falls in the vicinity of zero. However, on decreasing the value of  $\alpha$ , the Hilbert matrix

becomes severely ill-conditioned, and the performance of the competitive algorithms except *Gauss – Seidel* exhibit inconsistent behavior. The DCT performs better near  $\alpha = 1$  ( $-\log_{10}(\alpha) = 0$ ). This result is expected because diagonally dominant matrix behaves similar to a  $1^{st}$  order Markov process with  $\rho$  significantly small. However, the DCT shows inconsistency at  $\alpha = 0.001$ , where it again attains noticeable preconditioning of Hilbert matrix as opposed to other competitive methods.

We also evaluate our algorithm on five different random positive definite matrices with the values taken from a zero-mean and unit-variance Gaussian process. We regularize the matrices to ensure positive-definiteness. The results in Fig. 2(b) are bar-plotted. For example, the first bar corresponds to the results on the first random Gaussian positive definite matrix. Each bar is shown using six different colors corresponding to six methods. The width of each color is proportional to the condition ratio obtained by applying the corresponding preconditioning method. The condition numbers of the five positive definite matrices are 23.6, 31.8, 28.1, 26.5, and 269.1 respectively. The condition numbers that we obtain by applying PrecoG are 4.3, 3.1, 4.1, 4.2, and 17.5 respectively. It is evident from Fig. 2(b), the condition ratios obtained by applying PrecoG are at least 1.3 times better compared to DCT, and effectively well compared to Gauss-Seidel, DFT, and Jacobi.

The condition ratios (in  $\log_{10}$  scale) by applying PrecoG on sparse systems of equations are shown in Fig. 2(c). The five sparse matrices are random by construction with sparsity ( $\frac{\text{number of nonzero elements}}{\text{total number of elements}}$ ) levels as  $[\frac{5}{6}, \frac{2}{3}, \frac{1}{3}, \frac{1}{2}, \frac{1}{5}]$  respectively. For example,  $\frac{5}{6}$ th of all the entries in the first matrix which is symmetric and positive definite by construction, are nonzero. We present the experiments in decreasing order of sparsity with the most sparse one, in our experiment, containing only  $\frac{1}{5}$ th nonzero elements. The condition numbers of these matrices are 138.68, 1620, 22.88, 312.3, and 51.84. On applying PrecoG to these matrices, we obtain the corresponding condition numbers as 54.6, 491.94, 8.29, 81.8, and 22.3. From Fig. 2(c), it can be seen that PrecoG improves the condition numbers at least twice compared to DCT, DFT, Jacobi, incomplete

LU, and at least 1.4 times compared to Gauss-Seidel method.

*6.1. Comparison on 1<sup>st</sup> order Markov process and 2<sup>nd</sup> order autoregressive process*

The DCT is known as the near-optimal preconditioner for 1<sup>st</sup> and 2<sup>nd</sup> order Markov processes. The purpose of this section is to compare the preconditioning strength of our algorithm with that of DCT. We also include the strength of other methods as shown in the following figures.

First, we consider the autocorrelation matrix of a first order Markov process of signal correlation factor  $\rho$  ( $0 \leq \rho \leq 1$ ) [10]. The autocorrelation matrix,  $R_N(\rho)$  of such process is given in (1), which has a Toeplitz structure. Higher values of  $\rho$  indicate stronger correlation among data samples, which implies significantly higher eigenvalue spread of the autocorrelation matrix. Smaller  $\rho$  values imply weaker correlation among data instances, which is reflected in the diagonally-dominant structure of the input autocorrelation matrix  $R_N$ . It has been proved that the *DCT* is a near-optimal unitary transformation for this process. We compare our method against the DCT as presented in Fig. 3(a). Unlike other methods, our result exhibits a consistent behavior with respect to the DCT over different values of  $\rho$ . The fact that the condition ratios of other methods are nonlinearly increasing as the signal correlation factor approaches unity confirms the weaker performance of those methods compared to PrecoG.

In Fig. 3(b), we present the condition ratios computed by applying the algorithms on the autocorrelation matrices of eight 2<sup>nd</sup> order autoregressive process with parameters  $(\rho_1, \rho_2)$  [5]. The input autocorrelation matrix  $R_N$  of such process is given by  $R_N = c_1 R_N(\rho_1) + c_2 R_N(\rho_2)$ .  $R_N(\rho_1)$  and  $R_N(\rho_2)$  are two Toeplitz matrices, similar to  $R_N$  of 1<sup>st</sup> order Markov process.  $c_1$  and  $c_2$  are constants and are given by  $c_1 = \frac{\rho_1(1-\rho_2^2)}{(\rho_1-\rho_2)(1+\rho_1\rho_2)}$ ,  $c_2 = \frac{-\rho_2(1-\rho_1^2)}{(\rho_1-\rho_2)(1+\rho_1\rho_2)}$ . The values of the parameters  $(\rho_1, \rho_2)$  considered in the experiments are (0.015, 0.01), (0.15, 0.1), (0.75, 0.7), (0.25, 0.01), (0.75, 0.1), (0.9, 0.01), (0.95, 0.1), and (0.99, 0.7). Although the DCT provides a near-optimal option when the autocorrelation matrix is Toeplitz in nature, our approach is consistent and almost approximates

the DCT, while the others significantly deviate from the DCT in terms of the condition ratios.

*Comments:* With the condition ratio scores by the existing preconditioning techniques on different datasets at hand, it can be observed that the preconditioning capability of each method is essentially dataset-specific. For example, the DCT works significantly well for the Markov process, autoregressive process, whereas Gauss-Seidel exhibits better performances on preconditioning the *Hilbert* matrix and sparse linear systems. In all the aforementioned datasets except Markov process and autoregressive process, PrecoG shows its efficacy over other methods. For 1<sup>st</sup> order Markov process, 2<sup>nd</sup> order autoregressive process, PrecoG approximates the DCT in terms of the condition ratios. Therefore, it can be argued that if the input process is not known *a priori*, PrecoG can reduce the condition number and should be the preferred choice.

### 6.2. Performance by changing parameters

Next, we look at the performance of our algorithm in terms of condition ratio by varying a set of internal parameters - initialization of weights, number of iterations and length of the input vector. Fig. 4(a) shows the behavior of condition numbers for aforementioned datasets with five different initial weights,  $\mathbf{w}$ . It is evident that PrecoG yields better performance in the cases of Markov and autoregressive inputs compared to the remainder of the cases considered here. During experimentation, we obtained a few instances where PrecoG gives a substantial improvement not possible with existing techniques. For example, PrecoG achieves a condition number 10.64 in case of the Hilbert matrix as shown in Fig. 4(a).

Fig. 4(b) exhibits the result of the preconditioning capacity of PrecoG over iteration. For each dataset, we randomly initialize the weights and keep the input vector length as 10. There is a gradual decline in the trend of condition ratio for each dataset, which implies that PrecoG improves preconditioning over iteration.

Fig. 4(c) illustrates the consistent performance of PrecoG on the length of

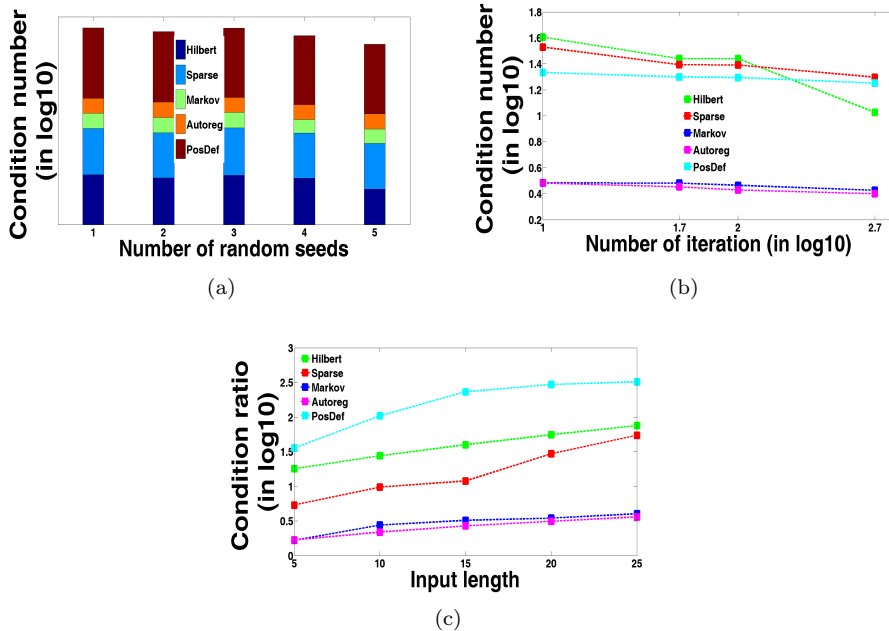


Figure 4: The performance of our algorithm on (a) different initialization of weights,  $\mathbf{w}$ , (b) the number of iterations for gradient descent, and (c) the length,  $N$  of input signal vector.

input vectors. There is a positive slope of the condition ratio with increments in the length of input vector. However, the results are shown using 15 iterations only. It is observed that PrecoG with longer input vector (larger graph) needs linearly more iterations to output better condition ratio.

## 7. Conclusion

In this letter, we present a method to obtain a unitary split preconditioner by utilizing nonconvex optimization and graph theory. We demonstrate the efficacy of our approach over prevalent state-of-the-art techniques. In addition, we show that our algorithm is amenable to precondition linear systems constrained with sparsity. As a future endeavor, we will attempt to exploit the signal structure and embed this structure into the optimization framework by including a set of constraints. In continuation, we will try to extend our approach to solve a sparse underdetermined linear system of equations in order to implement dictionary learning.

## Appendices

### Evaluation of $\left[\frac{\partial E(p)}{\partial U_N}\right]$

Let,  $M(\epsilon) = \|U^T R U - (1 + \epsilon)U^T R U \circ \mathcal{I}\|_F^2$ . Then,

$$M(\epsilon) = \text{Tr}\left(\{U^T R U - (1 + \epsilon)U^T R U \circ \mathcal{I}\} \{U^T R U - (1 + \epsilon)U^T R U \circ \mathcal{I}\}^T\right). \quad (15)$$

Eq. (15) on expansion gives

$$M(\epsilon) = \text{Tr}\left(U^T R^2 U - 2(1 + \epsilon)(U^T R U \circ \mathcal{I})(U^T R U) + (1 + \epsilon)^2(U^T R U \circ \mathcal{I})^2\right). \quad (16)$$

Eq. (16) is obtained using the fact that  $U U^T = \mathcal{I}$ . By performing the partial derivative,

$$\begin{aligned} \frac{\partial M(\epsilon)}{\partial U} &= \frac{\partial \text{Tr}(U^T R^2 U)}{\partial U} - 2(1 + \epsilon) \frac{\partial}{\partial U} \text{Tr}\{(U^T R U \circ \mathcal{I})(U^T R U)\} + (1 + \epsilon)^2 \frac{\partial}{\partial U} \text{Tr}(U^T R U \circ \mathcal{I})^2. \\ &= 2R^2 U - 4(1 + \epsilon)RU + (1 + \epsilon)^2(U^T R U \circ \mathcal{I})RU \end{aligned}$$

Next,  $\frac{\partial E(p)}{\partial U}$  is computed using  $\frac{\partial M}{\partial U}$  as  $\frac{\partial E(p)}{\partial U} = \frac{\partial M(+\epsilon_1)}{\partial U} + \frac{\partial M(-\epsilon_2)}{\partial U}$ .

$$\begin{aligned} \frac{\partial E(p)}{\partial U_n} &= 2\left[2R_n - 2(2 - \epsilon_2 - \epsilon_2)\mathcal{I} - \{(1 + \epsilon_1)^2 + (1 - \epsilon_2)^2\}U_n^T R_n U_n \circ \mathcal{I}\right]R_n U_n. \end{aligned} \quad (17)$$

If  $\epsilon_1 = \epsilon_2$ , the above expression can be simplified as

$$\begin{aligned} \frac{\partial E(p)}{\partial U_n} &= 4\left(R_n - (1 - \epsilon)\mathcal{I} - (1 + \epsilon^2)U_n^T R_n U_n \circ \mathcal{I}\right)R_n U_n \end{aligned} \quad (18)$$

## References

- [1] B. Widrow, M. E. J. Hoff, Adaptive switching circuits., in: 1960 IRE WESCON Convention record: at the Western Electronic Show and Convention, Los Angeles, Calif., August 23-26, 1960, Institute of Radio Engineers, 1960.
- [2] C. Paleologu, S. Ciochina, A. A. Enescu, C. Vladeanu, Gradient adaptive lattice algorithm suitable for fixed point implementation, in: Digital Telecommunications, 2008. ICDT'08. The Third International Conference on, IEEE, 2008, pp. 41–46.
- [3] H. Fan, X. Q. Liu, Gal and lsl revisited: new convergence results, IEEE transaction on signal processing 41 (1) (1993) 55–66.
- [4] S. Haykin, Adaptive Filter Theory (3rd Ed.), Prentice-Hall, Inc., Upper Saddle River, NJ, USA, 1996.
- [5] S. Zhao, Z. Man, S. Khoo, H. R. Wu, Stability and convergence analysis of transform-domain lms adaptive filters with second-order autoregressive process, Signal Processing, IEEE Transactions on 57 (1) (2009) 119–130.
- [6] S. Hosur, A. H. Tewfik, Wavelet transform domain adaptive fir filtering, Signal Processing, IEEE Transactions on 45 (3) (1997) 617–630.
- [7] M. H. Costa, J. C. M. Bermudez, N. J. Bershad, Stochastic analysis of the lms algorithm with a saturation nonlinearity following the adaptive filter output, Signal Processing, IEEE Transactions on 49 (7) (2001) 1370–1387.
- [8] D. I. Kim, P. De Wilde, Performance analysis of the dct-lms adaptive filtering algorithm, Signal Processing 80 (8) (2000) 1629–1654.
- [9] B. Farhang-Boroujeny, Transform domain adaptive filters, Adaptive Filters: Theory and Applications (1998) 207–250.
- [10] F. Beaufays, Transform-domain adaptive filters: an analytical approach, Signal Processing, IEEE Transactions on 43 (2) (1995) 422–431.

- [11] K. Chen, Matrix preconditioning techniques and applications, Vol. 19, Cambridge University Press, 2005.
- [12] M. Benzi, Preconditioning techniques for large linear systems: a survey, *Journal of computational Physics* 182 (2) (2002) 418–477.
- [13] Y. Cao, M.-Q. Jiang, Y.-L. Zheng, A splitting preconditioner for saddle point problems, *Numerical Linear Algebra with Applications* 18 (5) (2011) 875–895.
- [14] Q. Zheng, L. Lu, Extended shift-splitting preconditioners for saddle point problems, *Journal of Computational and Applied Mathematics* 313 (2017) 70–81.
- [15] Y. Dauphin, H. de Vries, Y. Bengio, Equilibrated adaptive learning rates for non-convex optimization, in: *Advances in Neural Information Processing Systems*, 2015, pp. 1504–1512.
- [16] O. Chapelle, D. Erhan, Improved preconditioner for hessian free optimization, in: *NIPS Workshop on Deep Learning and Unsupervised Feature Learning*, Vol. 201, 2011.
- [17] A. Dziekonski, A. Lamecki, M. Mrozowski, Jacobi and gauss-seidel preconditioned complex conjugate gradient method with gpu acceleration for finite element method, in: *Microwave Conference (EuMC), 2010 European*, IEEE, 2010, pp. 1305–1308.
- [18] W.-P. Tang, Toward an effective sparse approximate inverse preconditioner, *SIAM journal on matrix analysis and applications* 20 (4) (1999) 970–986.
- [19] M. Benzi, J. K. Cullum, M. Tuma, Robust approximate inverse preconditioning for the conjugate gradient method, *SIAM Journal on Scientific Computing* 22 (4) (2000) 1318–1332.
- [20] E. Chow, A. Patel, Fine-grained parallel incomplete lu factorization, *SIAM Journal on Scientific Computing* 37 (2) (2015) C169–C193.

- [21] H. P. Margetic, D. Thanou, P. Frossard, Graph learning under sparsity priors, in: *Acoustics, Speech and Signal Processing (ICASSP)*, 2017 IEEE International Conference on, Ieee, 2017, pp. 6523–6527.
- [22] E. Pavez, H. E. Egilmez, A. Ortega, Learning graphs with monotone topology properties and multiple connected components, *IEEE Transactions on Signal Processing*.
- [23] M. G. Rabbat, Inferring sparse graphs from smooth signals with theoretical guarantees, in: *Acoustics, Speech and Signal Processing (ICASSP)*, 2017 IEEE International Conference on, IEEE, 2017, pp. 6533–6537.
- [24] J. Abernethy, O. Chapelle, C. Castillo, Graph regularization methods for web spam detection, *Machine Learning* 81 (2) (2010) 207–225.
- [25] O. Lezoray, V. T. Ta, A. Elmoataz, Nonlocal graph regularization for image colorization, in: *Pattern Recognition, 2008. ICPR 2008. 19th International Conference on*, IEEE, 2008, pp. 1–4.
- [26] H. Bunke, K. Riesen, Recent advances in graph-based pattern recognition with applications in document analysis, *Pattern Recognition* 44 (5) (2011) 1057–1067.
- [27] D. Hallac, J. Leskovec, S. Boyd, Network lasso: Clustering and optimization in large graphs, in: *Proceedings of the 21th ACM SIGKDD international conference on knowledge discovery and data mining*, ACM, 2015, pp. 387–396.
- [28] V. Kalofolias, How to learn a graph from smooth signals, in: *Artificial Intelligence and Statistics*, 2016, pp. 920–929.
- [29] M.-D. Choi, Tricks or treats with the hilbert matrix, *The American Mathematical Monthly* 90 (5) (1983) 301–312.